

Multi-scale Nonlinear Turbulence Dynamics Studies

G.R. Tynan 1), P.H. Diamond 2) , O. Gurcan 2) , C. Holland 1) , S.H. Muller 1) , M. Xu 1), Z. Yan 1), J. Yu 1), P. Manz 3), M. Ramisch 3), U. Stroth 3), Y. Nagashima 4) , S.I. Itoh 4) , M. Yagi 4), S. Inagaki 5) , A. Fujisawa 5), N. Kasuya 5), K. Itoh 5), T. Windisch 6), O. Grulke 6), T. Klinger 6),

- 1) Center for Energy Research, UCSD, La Jolla CA, USA
- 2) Center for Astrophysics and Space Science, UCSD, La Jolla CA, USA
- 3) Institute for Plasma Research, Univ. Stuttgart, Germany
- 4) Research Institute for Applied Mechanics, Kyushu University, Fukuoka Japan,
- 5) National Institute for Fusion Science, Toki, Japan
- 6) Max Planck Institute for Plasma Physics, Euratom Association, Greifswald, Germany

Email contact of main author: gtynan@ucsd.edu

1.0 Introduction

Critical gradient transport dynamics, breaking of gyro-Bohm transport scaling, transport bifurcation, and transport barrier formation all have a profound effect on confinement in magnetic fusion devices, and are thought to be both generated and regulated by the nonlinear interaction between gradient-driven small scaled ($k_{\perp}\rho_s < 1$) drift turbulence and larger meso-scaled structures such as zonal flows and streamers with $k_{\perp}\rho_s \ll 1$ [1, 2] that are generated from the turbulence. Zonal flow formation from turbulence, regulation of the turbulence by the zonal flow, effects of flow damping rate on turbulence saturation, and introduction of device-scaled transport events due to the breakdown of zonal flows and formation of propagating structures are *the* key nonlinear physics processes that lead to these macroscopic confinement properties. Direct study of the underlying physics requires simultaneous spatiotemporal turbulence measurements that cannot be made in existing large confinement devices. Suitably designed and diagnosed smaller laboratory experiments such as the TJ-K toroidal device and the CSDX, VINETA, and LMD linear devices have recently provided direct experimental study of these issues, and thus provide a detailed stress test of theory and simulation.

2.0 Multifield Nonlinear Drift Turbulence Energy Transfer:

Experiments on TJ-K are providing the first k-space resolved measurements of the transfer of kinetic energy, $\propto k_{\perp}^2 \tilde{\phi}_k^2$, and internal energy, $\propto \tilde{n}_k^2$ due to the nonlinear dynamics of drift turbulence, and allow comparison of this fundamental quantity against simulation of electrostatic drift turbulence [3]. Measurement of the density fluctuations $\tilde{n}(r, \theta, t)$ or the potential fluctuations $\tilde{\phi}(r, \theta, t)$ in the poloidal plane are used to compute the energy transfer from a one-field model of drift wave turbulence valid when the normalized parallel electron dissipation rate $C \equiv \frac{k_{\parallel}^2 v_{the}^2}{\omega \nu_e}$ is large [4]. The experimental results (*Figure 1* Right panels)

show the existence of a dual energy transfer process, where the internal energy ($\propto \tilde{n}^2$) is nonlinearly transferred to large wavenumber ($k_{\perp}\rho_s > 1.5$) and the kinetic energy ($\propto (k_{\perp}\tilde{\phi})^2$) is simultaneously transferred to small wavenumber ($k_{\perp}\rho_s < 1.5$) in a confined toroidal

plasma [2] with $C \approx 1$ which is close to the value found in fusion edge plasmas. The validity of this approach has been tested on simulated data from a Hasegawa-Wakatani code that solves the advection of density and vorticity due to the drift turbulence ExB drifts [5]. Simulation results for a higher value $C=2$ (*Figure 1* left panels) show that the spectral energy transfer of the density fluctuations follows that of the potential fluctuations; in this case both are transferred to larger spatial scales in contrast to the experimental results. Simulations with $C=1$ show that the density fluctuation power is transferred to smaller spatial scales while the kinetic energy is transferred to larger scaled in reasonable agreement with experiment.

3.0 Zonal Flows Generation from Turbulence

Zonal flows, which are radially sheared plasma ExB flows within a flux surface that are driven by the transfer of turbulent kinetic energy into the shear flow via the turbulent Reynolds stress, are thought to play a crucial role in regulating the magnitude of drift turbulence and the associated rate of particle, momentum, and heat transport across the magnetic field [1, 2]. Confinement experiments have demonstrated their essential elements [6, 7]. In the CSDX device, a turbulent driven zonal flow has been observed directly for the first time using a fast camera that is observing parallel to the magnetic field to record the motion of the visible light fluctuations associated with collisional drift turbulence. A time-delay analysis [8] of the fluctuation propagation then provides a direct measure of the radially sheared flow field (*Figure 2*) which has also been shown to be associated with a bulk fluid flow [9]. By directly measuring the turbulent Reynolds stress and the ensemble averaged azimuthal flow radial profile and estimating the linear flow damping mechanisms, the sheared flow has been shown to be self-consistent with the turbulent momentum conservation in a linear laboratory device [10, 11] (see *Figure 3*), consistent with expectations for a turbulent driven zonal flow.

3.1 Turbulent Structure Evolution and Barrier Formation by a Zonal Flow:

The transfer of internal energy observed in TJ-K is manifested in configuration space by the shearing apart of turbulent structures immersed in the zonal flow – the essential shear decorrelation process that leads to transport barrier formation [12]. The spatial evolution of turbulent structures has been directly visualized by the same fast imaging diagnostic on CSDX that was used to visualize the zonal flow shown above. A representative example is shown in *Figure 4*. Positive visible light excursions (corresponding to a combination of increased plasma density and electron temperature) are highlighted by the green ellipses in the figure. Two such excursions are observed to merge early on (frames (a-c)). As the structure grows in magnitude and approaches the shear layer location (denoted by the dashed black line near $r \sim 4$ cm) the structure develops an azimuthally elongated shape (frames (c-e)). Eventually the structure becomes highly elongated azimuthally, and the radial scale length of the structure is decreased from ~ 2 cm to less than 1 cm. Late in time (frame (f)) the structure appears to be “trapped” at the shear layer, resulting in the formation of a turbulent particle flux transport barrier as has been shown elsewhere [13] by measurements of the correlated density and radial velocity fluctuations.

4.0 Observation of Streamer-like Mesoscale Structures

In addition to the formation of zonal flows, nonlinear interactions of drift waves can lead to the formation of radially elongated azimuthally (or poloidally) localized structures denoted

as streamers. Evidence for such structures has been shown in the LMD linear device; the key results are shown in *Figure 5a* below. In this work, spatially distributed probe arrays were used to show the simultaneous existence of multiple nonlinearly interacting drift wave and interchange modes. This interaction was shown to lead to the transient formation of a streamer-like structure that extends over the entire plasma column due to the nonlinear interaction of drift waves at other frequencies – the essential nonlinear element that leads to the emergence of the elongated structure. This structure is immersed within smaller scaled drift wave structures as shown in *Figure 5b*. Clearly such elongated structures can have a significant effect on the rate of cross-field transport in confined plasmas.

5.0 Mesoscale Structure Selection Mechanism

Results from LMD have also shown evidence for a turbulent-driven shear flow (i.e. a zonal flow) much like the observations summarized above from the CSDX laboratory device [14]. Thus the question naturally arises: What determines the selection of the type of mesoscale structure (i.e. zonal flows vs. streamers) that forms? This question strikes at the heart of the quality of confinement of magnetically confined plasmas, and is also germane to how the turbulent scale length varies with system size (i.e. the Bohm vs. gyro-Bohm transport scaling). This question has been studied with a three-field reduced fluid model, which is extended to describe the resistive drift wave turbulence in magnetized cylindrical plasmas [15, 16]. There are multiple energy exchange paths included in the model, resulting in the existence of two kinds of nonlinear steady states in simulations with a fixed particle source: one dominated by a zonal flow generated by modulational coupling of various unstable modes, which suppress transport, and the other state dominated by a streamer, which is an azimuthally-localized radially elongated vortex structure that effectively induces convective transport down the mean gradients, and which is formed by parametric coupling with other fluctuation components. Simulation results suggest that the selection is controlled by the damping rate of the zonal flow, which in the case of the LMD experiments is due to ion-neutral collision frequency (*Figure 6*). This prediction needs to be tested experimentally; such work is planned for upcoming experiments. It is important to note that the form of the ion-neutral damping (i.e. that of a drag term that is proportional to ion flow speed) is similar to the damping that is expected from ion-ion collisional damping of zonal flows in a torus. Thus perhaps a similar transition between zonal flow dominated mesoscale and streamer dominated mesoscale feature might be expected. The answer to this speculation requires further experimental study.

6.0 Formation of radially propagating structures

Experiments on the VINETA device, which is similar to both the CSDX and LMD devices, allow the study of the formation of radially propagating coherent structures (also referred to as blobs, avaloids, or intermittent plasma objects in the literature). In these experiments [17] a reference probe is used to monitor the density fluctuations at the boundary of the central portion of the cylindrical plasma (denoted by the filled black dot in *Figure 7*, and a movable probe is then used to sample the density fluctuations in the two-dimensional plane perpendicular to the magnetic field. A conditional averaging technique is then used to map out the two-dimensional correlation function from the density fluctuations for different delay times. The results (*Figure 7*) show that, on average, the blobs are formed by peeling off a portion of plasma from the boundary of a large-amplitude $m=1$ density perturbation that exists in the core region of the plasma. This new blob structure then propagates radially away from the core plasma; the azimuthal propagation direction of the blob is also reversed

relative to the central plasma region, indicating that some type of velocity shearing process is occurring at the the outer region of the plasma. For the conditions of these experiments, the published results do not suggest that the zonal flows studied in the CSDX and LMD devices is present in the VINETA plasma. The formation of blobs in the presence of a zonal flow is a topic for future work.

7.0 Concluding Comments

These results directly confirm the physics of zonal flow formation from turbulence, regulation of the radial scale length and decorrelation of turbulence by the zonal flow, formation of non-diffusive transport events via nonlinear processes, the existence of dual energy transfer processes for kinetic energy and density fluctuations. These physical processes form the physics basis for important confinement processes such as gyro-Bohm breaking, critical gradient transport scaling, and transport barrier formation in magnetic fusion confinement devices. The observations also demonstrate the universal nature of these processes, independent of the detailed confinement geometry. Because of this universality and the availability of detailed spatio-temporal measurements of turbulence in such experiments, detailed studies of the nonlinear drift turbulence dynamics of magnetically confined plasmas and validation of first principles simulation are now possible.

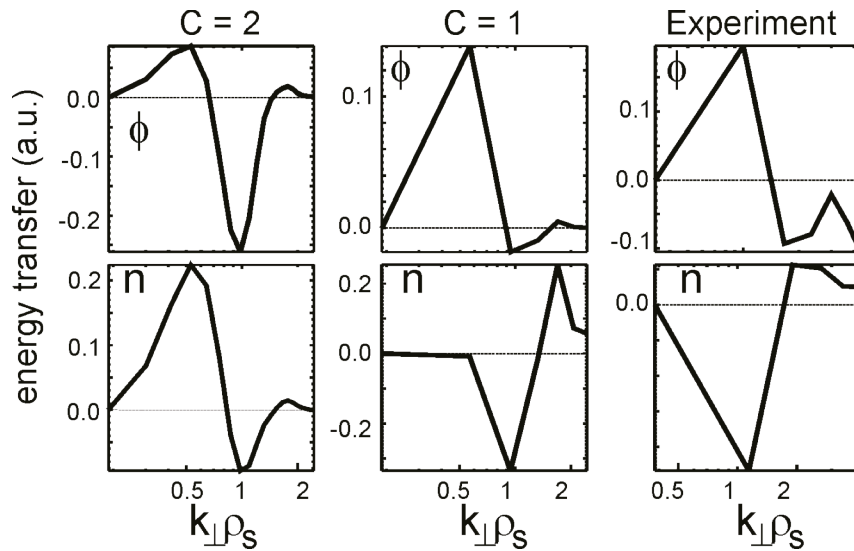


Figure 1: Left: Nonlinear energy transfer for kinetic energy (upper) and density (lower) in weakly dissipative collisional drift turbulence simulation with $C=2$. Center: Simulation results for $C=1$ (equivalent to experimental conditions). Right: Experimental results show dual cascade in qualitative agreement with $C=1$ simulation results; kinetic energy is transferred preferentially to small $k_{\perp}\rho_s$, while internal energy is transferred to high $k_{\perp}\rho_s$. Figure adapted from results contained in [3].

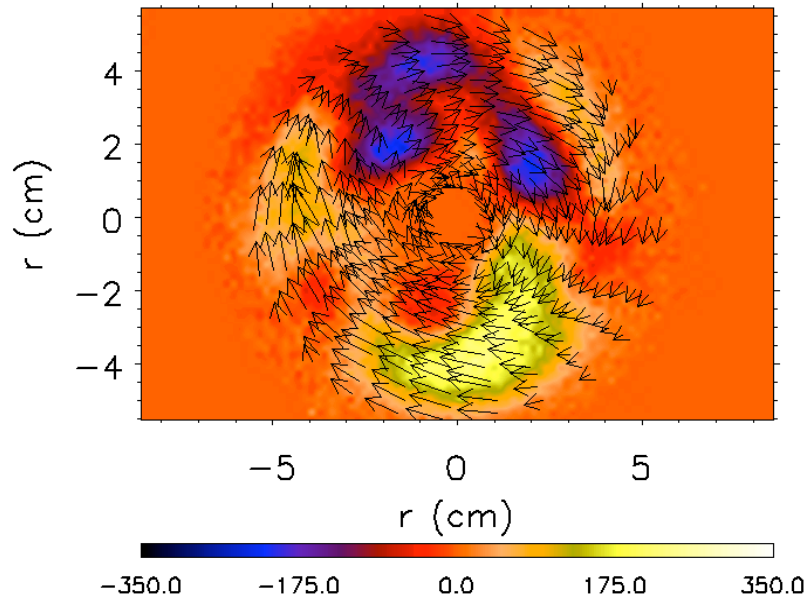


Figure 2: Instantaneous flow field in the plane perpendicular to the magnetic field inferred from motion of visible light intensity fluctuations associated with collisional drift turbulence in the CSDX device. A radially sheared azimuthal flow exists with a peak shearing rate near $r \sim 3.5\text{-}4.0\text{cm}$; the flux-surface averaged ensemble-averaged shear flow is consistent with the turbulent momentum balance analysis. The secondary objective of the telescope blocks the $r < 1.0\text{cm}$ region. Data obtained from CSDX for 0.1T 3.0mTorr Argon 1.5kW with 100kHz framing rate.

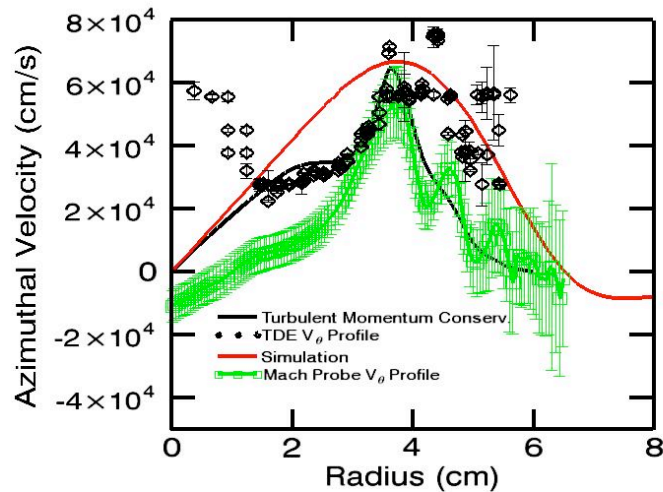


Figure 3: Radial profiles of measured and predicted azimuthal flow in the CSDX device. Green data points: Mach probe measurement of ion fluid flow. Black open diamonds: Time-delay estimation measurement of turbulent group velocity. Black solid line: Mean flow expected from turbulent momentum balance analysis. Red solid line: Result predicted from Hasegawa-Wakatani drift turbulence simulation. Figure reproduced from [10] "Observation of turbulent-driven shear flow in a cylindrical laboratory plasma device," by G.R. Tynan et al, *Plas. Phys. Cont. Fusion* 48 S51-S73 (2006), published by IOP and reproduced with permission.

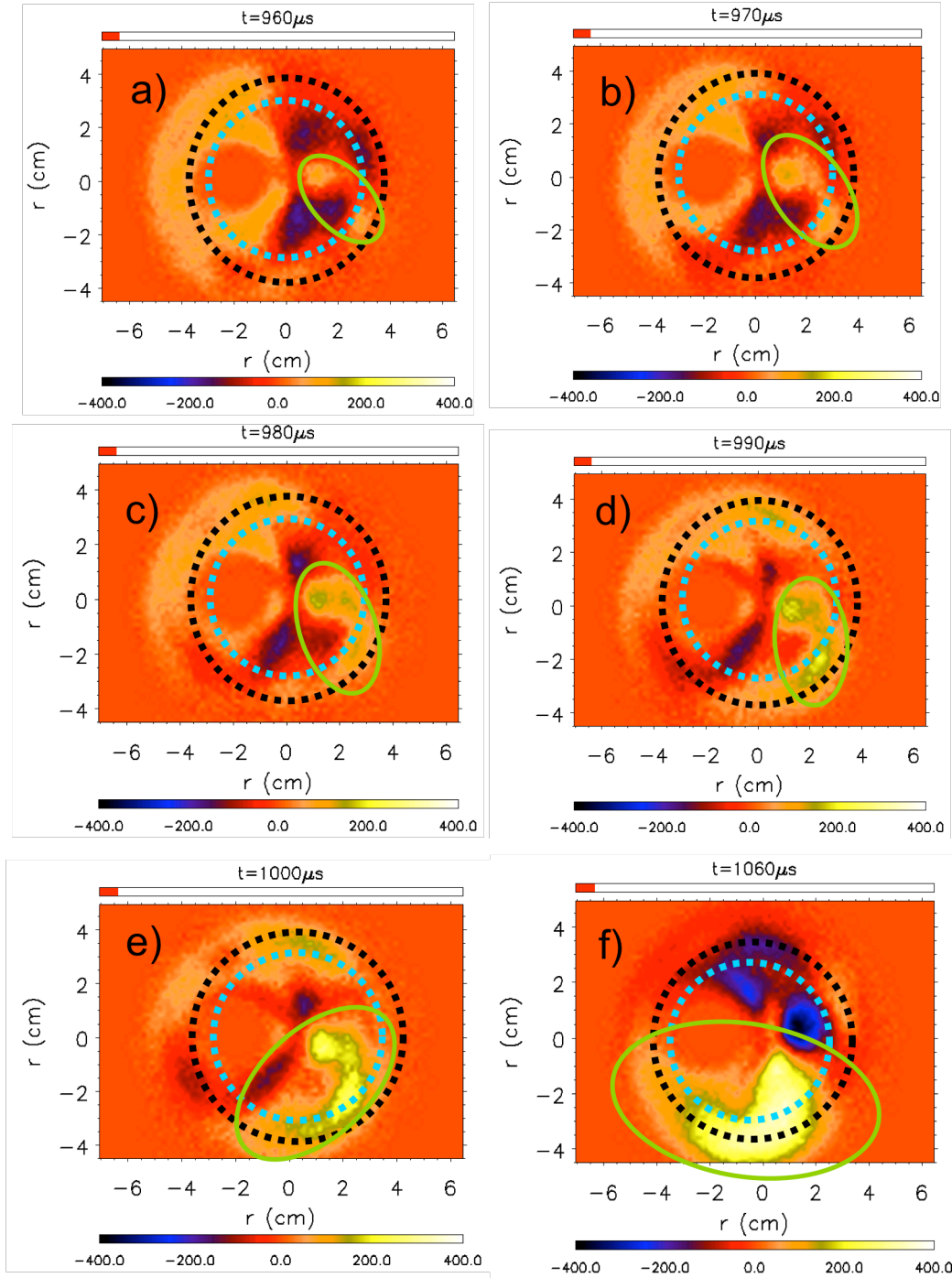


Figure 4: Evolution of visible light emission fluctuations from collision drift turbulence driven by the peak pressure gradient located at the dashed blue line. Positive fluctuations identified by the heavy solid green ellipse, forms and merge in frames (a)-(c). The structure is azimuthally distended, and grows in amplitude (frames c-e). Later in time (frame f) the structure is located at the shear layer (denoted by black dotted circle) but does not penetrate outward beyond the shear layer. The secondary objective of the telescope blocks light over a $\sim 3\text{cm}$ region centered at $x=-2\text{cm}$ $y=0\text{cm}$. Data obtained from CSDX for 0.1T 3.0mTorr Argon 1.5kW with 100kHz framing rate.

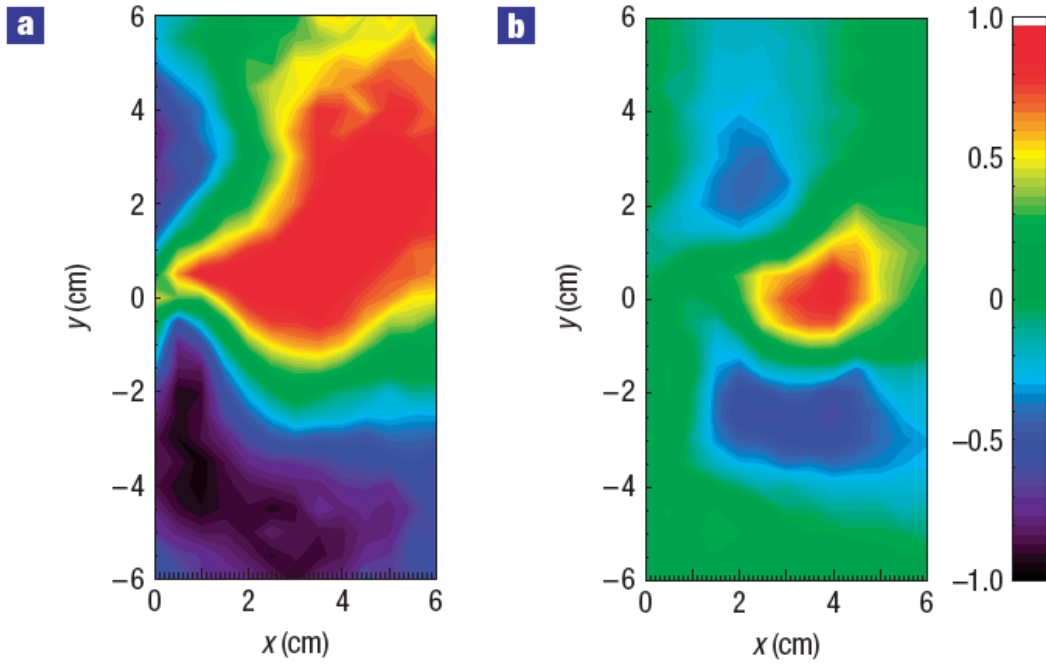


Figure 5 Real part of ion saturation current cross-spectra computed between reference probe located at $x=4.0\text{cm}$, $y=0\text{cm}$ and a probe movable in the x - y plane transverse to magnetic field. (a) a radially elongated streamer-like structure at 7.8 kHz is formed in the LMD device due to the nonlinear interaction of other drift wave components. (b) broadband residual wave-like density perturbations over the range 10-15 kHz. Figure reproduced from reference [18], Nature Physics article number doi:10.1038/nphys1029 with permission.

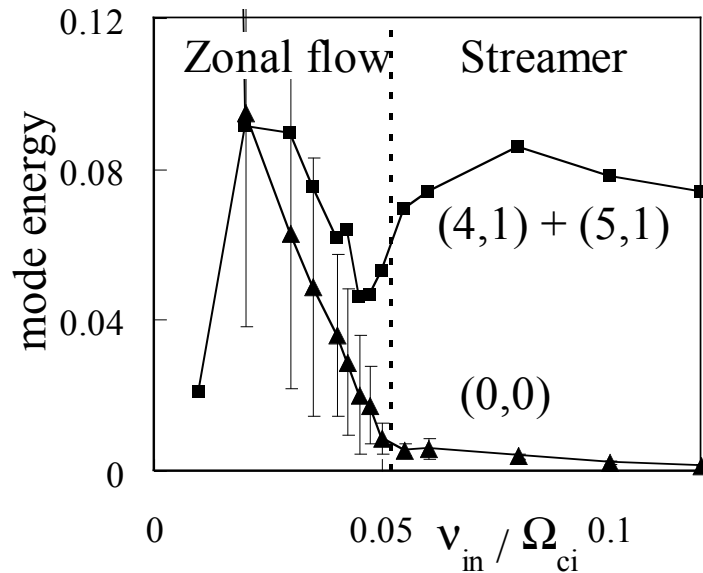


Figure 6: Dependencies of the energies of fluctuations (square) and of zonal flow (triangle) on v_{in} in nonlinear steady states. Streamers dominate the dynamics at higher damping rates. Results adapted from simulations contained in [15, 16].

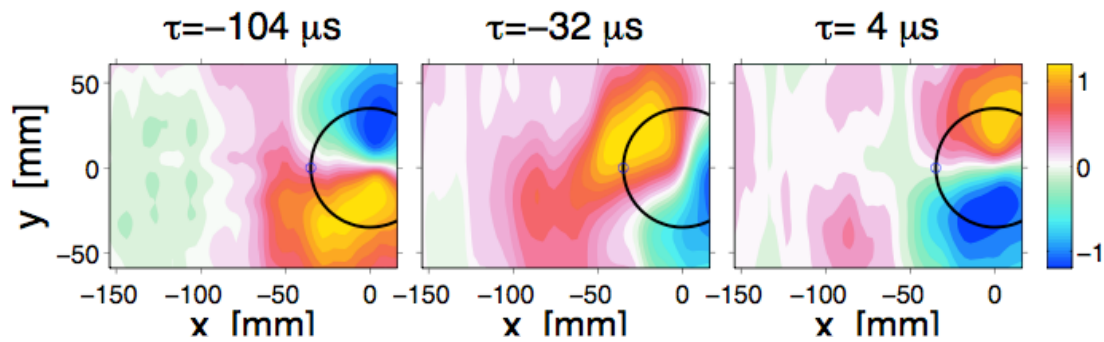


Figure 7: Conditionally averaged amplitude of density perturbations in the VINETA device for three different observation times. Reference point is shown as the filled black dot at $y=0\text{mm}$ $x=-40\text{mm}$. An intermittent density structure (“blob”) forms on the periphery of an $m=1$ density perturbation located in the central plasma region ($r<40\text{mm}$). Differential rotation of the plasma peels or shears this blob away from the main plasma column, forming a detached density structure. Results adapted from [17].

REFERENCES

- [1] P. H. Diamond *et al.*, Plasma Phys. Control. Fusion **47**, R35 (2005).
- [2] K. Itoh *et al.*, Phys. Plasmas **13**, 11 (2006).
- [3] P. Manz *et al.*, Plasma Phys. Control. Fusion **50** (2008).
- [4] J. S. Kim *et al.*, Phys. Plasmas **3**, 3998 (1996).
- [5] A. Hasegawa, and M. Wakatani, Phys. Rev. Lett. **50**, 682 (1983).
- [6] A. Fujisawa *et al.*, Phys. Rev. Lett. **93**, 4 (2004).
- [7] D. K. Gupta *et al.*, Phys. Rev. Lett. **97**, 4 (2006).
- [8] C. Holland *et al.*, Rev. Sci. Instrum. **75**, 4278 (2004).
- [9] J. H. Yu *et al.*, J. Nucl. Mater. **363**, 728 (2007).
- [10] G. R. Tynan *et al.*, Plasma Phys. Control. Fusion **48**, S51 (2006).
- [11] C. Holland *et al.*, Phys. Rev. Lett. **96**, 4 (2006).
- [12] H. Biglari, P. H. Diamond, and P. W. Terry, Physics of Fluids B-Plasma Physics **2**, 1 (1990).
- [13] M. J. Burin *et al.*, Phys. Plasmas **12**, 14 (2005).
- [14] Y. Nagashima, submitted to Phys. Rev. Lett. (private communication) (2008).
- [15] N. Kasuya *et al.*, J. Phys. Soc. Jpn. **76**, 12 (2007).
- [16] N. Kasuya, M. Yagi, and K. Itoh, J. Plasma Phys. **72**, 957 (2006).
- [17] T. Windisch, O. Grulke, and T. Klinger, Phys. Plasmas **13**, 7 (2006).
- [18] T. Yamada, Nature Physic article doi 10.1038/nphys1029 (2008).